ACS NANO
Cite This: ACS Nano XXXX, XXX, XXX−XXX
www.acsnano.org

ARTICLE

Colorimetric Paper-Based Immunosensor for Simultaneous Determination of Fetuin B and Clusterin toward Early Alzheimer's Diagnosis

Laís C. Brazaca,*[†][‡] José R. Moreto,[§] Aída Martín,[‡] Farshad Tehrani,[‡] Joseph Wang,[‡] and Valtencir Zucolotto*[†]

[†]Nanomedicine and Nanotoxicology Group, São Carlos Institute of Physics, University of São Paulo, 13560-970 São Carlos, SP, Brazil

[‡]Department of NanoEngineering, University of California, San Diego, La Jolla, California 92093, United States

[§]Department of Aerospace Engineering, San Diego State University, San Diego, California 92182-1308, United States

Supporting Information

ABSTRACT: **Alzheimer's disease is a devastating condition characterized by a progressive and slow brain decay in elders. Here, we developed a paper-based lateral flow immunoassay for simultaneous and fast determination of Alzheimer's blood biomarkers, fetuin B and clusterin. Selective antibodies to targeted biomarkers were immobilized on gold nanoparticles (AuNPs) and deposited on paper pads. After adding the sample on the paper-based device, the biofluid laterally flows toward the selective antibody, permitting AuNP-Ab accumulation on the test zone, which causes a color change from white to pink. Image analysis was performed using a customized algorithm for the automatic recognition of the area of analysis and color clustering. Colorimetric detection was compared to electrochemical methods for the precise quantification of biomarkers. The best performance was found for the color parameter "*L**". Good linearity (R^2 = 0.988 and 0.998) and reproducibility (%RSD = 2.79% and 1.82%, N = 3) were demonstrated for the quantification of fetuin B and clusterin, respectively. Furthermore, the specificity of the immunosensor was tested on mixtures of proteins, showing negligible cross-reactivity and good performance in complex environments. We believe that our biosensor has a potential for early-stage diagnosis of Alzheimer's disease and toward a better understanding of Alzheimer's developing mechanisms.**

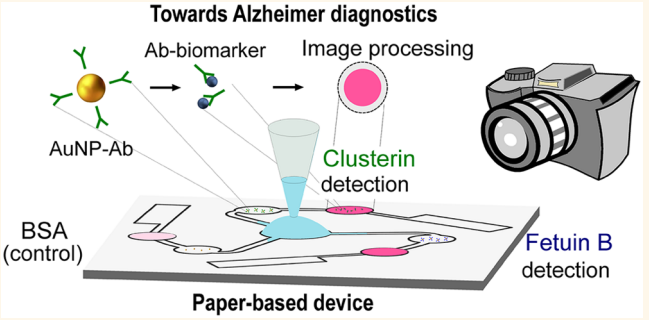

KEYWORDS: *Alzheimer's diagnosis, immunosensor, colorimetry, electrochemical detection, fetuin B, clusterin*

Alzheimer's disease (AD) is a neurodegenerative illness characterized by a progressive and irreversible decline on diverse intellectual functions such as memory, orientation in time and space, and ability to perform daily tasks.[1] Currently, there is not a unique simple test for precise diagnosis of AD. Accordingly, neuroimaging of the brain and analysis of target biomarkers in cerebrospinal fluid (CSF) are performed.[1,2] Such diagnostic methods are poorly accessible, time-consuming and require specialized professionals and costly equipment. Furthermore, CSF analysis involves a highly invasive lumbar puncture, presenting an extremely negative perception to the public.[3,4] Additionally, successive CSF sampling is limited, as it can impact biomarkers levels.[5]

Consequently, recent efforts have been focused on the identification of AD biomarkers in the blood.[6] Advantages in replacing blood over CSF include easy and low-cost sampling, which allows tests to be performed more frequently in a greater number of patients. Although a unique biomarker capable of diagnosing AD with high fidelity has yet to be discovered, the detection of multiple biomolecules appears to be a promising approach. Among them, altered concentrations of proteins such as fetuins and clusterin have been reported in the literature to be related with AD disease.[8−10] Fetuin B and fetuin A display lower blood concentrations in AD patients when compared to healthy subjects, being mainly related to brain volume.[8,9] Clusterin, on the other hand, presents itself in higher blood concentrations in AD patients, being possibly related to the cognitive decline rate.[8,9,10] Typical plasma concentrations are on the order of 10^{-2} g/L or 0.2 μmol/L[11,12] and 10^{-3} g/L or 10 nmol/L,[13] for

Received: August 19, 2019
Accepted: October 29, 2019
Published: October 29, 2019

Downloaded via UNIV OF SAO PAULO on November 7, 2019 at 11:18:05 (UTC).
See https://pubs.acs.org/sharingguidelines for options on how to legitimately share published articles.

© XXXX American Chemical Society

DOI: 10.1021/acsnano.9b06571
ACS Nano XXXX, XXX, XXX−XXX

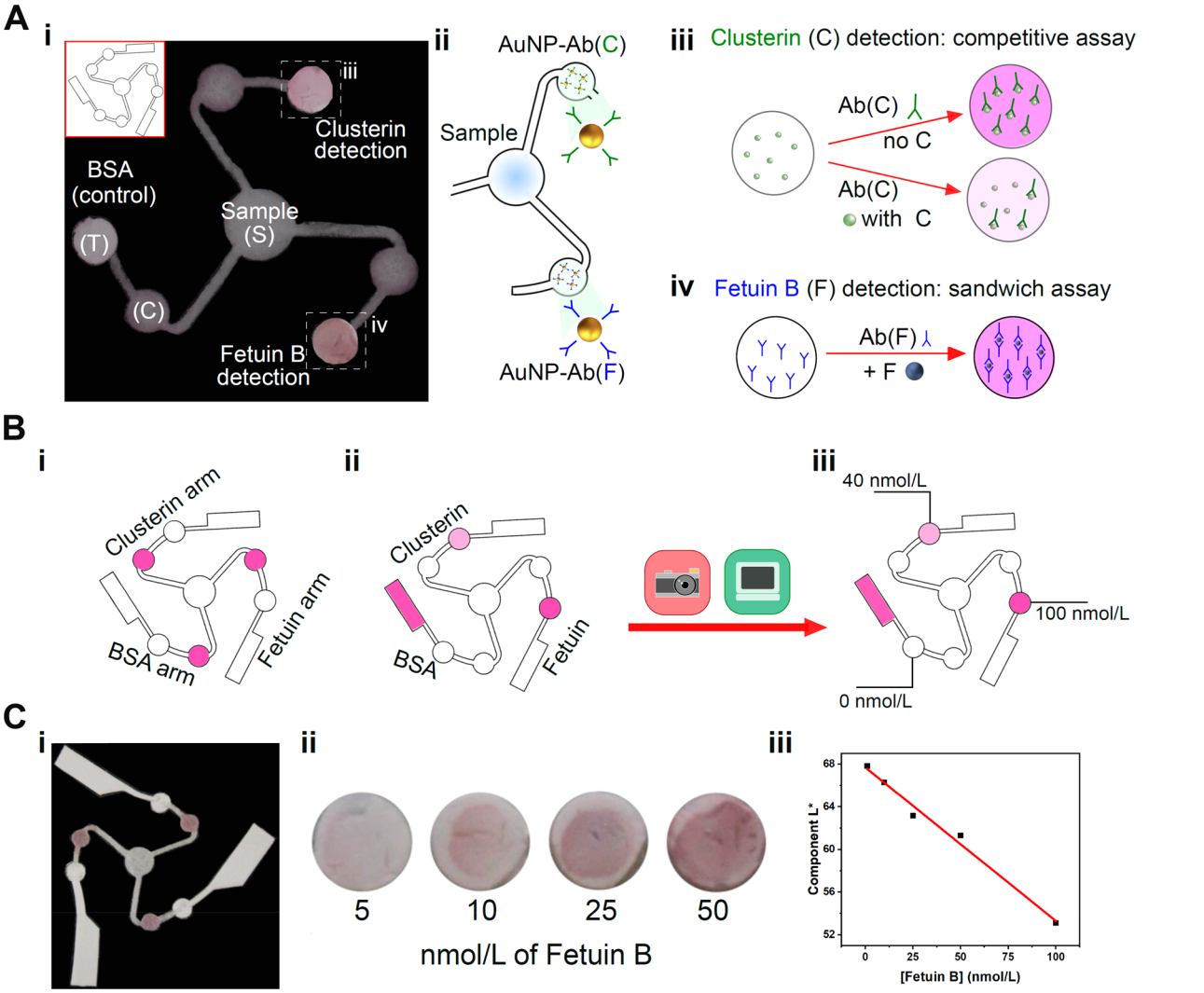

Figure 1. (A) (i) Lateral flow paper device for the detection of clusterin and fetuin B including sample (S), conjugation (C), and test (T) areas. (ii) Before sample addition, selective antibodies to clusterin (Cl) and fetuin B (F) immobilized on AuNPs were loaded on the conjugation zone. (iii) Strategy followed to detect clusterin was based on a competitive assay in which clusterin immobilized on the test zone competes for the AuNP-Ab with the protein present in the sample. (iv) Sandwich strategy used for detection of fetuin B relying on the antibody immobilization on the test zone and combination of analyte and AuNP-Ab on this zone. Two independent arms are used for the simultaneous detection of Alzheimer's disease biomarkers clusterin and fetuin B, while the third arm is used as a negative control (BSA). (B) Colorimetric analysis of lateral flow assays. Color distribution (i) before and (ii) after sample addition. Part ii also shows the colorimetric analysis using an automated Matlab software. (C) (i) Device picture. (ii) Sample data. Color changes in the test zone upon the addition of different fetuin B concentrations. (iii) Calibration curve constructed using the colorimetric component L^* on $L^*a^*b^*$ color space.

fetuin B and clusterin, respectively. Although the relation of these proteins with the disease is well established by many researchers, still there is not a complete study that includes the specific values from which AD can be diagnosed among different patient groups. Current quantification of these biomarkers within blood is performed by enzyme-linked immunosorbent assay (ELISA), which, although being precise and presenting low limits of detection (LOD), requires specialized researchers and equipment, presenting high costs and low portability and availability. Therefore, the development of deployable, low-cost, and accessible techniques for quantifying AD blood biomarkers is of great interest for advancement and further study of early detection of the illness.

Microfluidic paper-based analytical devices (μPADs) have emerged as a promising clinic-based diagnostic platform for the development of simple, portable, and low-cost devices for multiple biomarker quantification.[14−17] The combination of μPADs with colorimetric and electrochemical detection has demonstrated selectivity and multiplexing capabilities of this method toward early detection of different diseases.[18−20]

Herein, we describe a paper-based lateral flow immunoassay for the simultaneous, fast, and low-cost determination of Alzheimer's blood biomarkers, fetuin B and clusterin. The microfluidic device comprises four pads (sample, conjugate, test, and absorbent pads). Selective antibodies to targeted biomarkers were immobilized on gold nanoparticles (AuNPs) and deposited on the conjugate pads. After adding the biofluid on the paper-based device, it laterally flows toward the selective bioreceptors, allowing AuNPs to accumulate on the test zone. The quantification of biomarkers was evaluated by the analysis of the color intensity on the test zone and by measuring the oxidation peaks of AuNPs *via* stripping voltammetry measurements. Both colorimetric and electrochemical detections have been evaluated and compared for both biomarkers. Finally,

DOI: 10.1021/acsnano.9b06571
ACS Nano XXXX, XXX, XXX−XXX

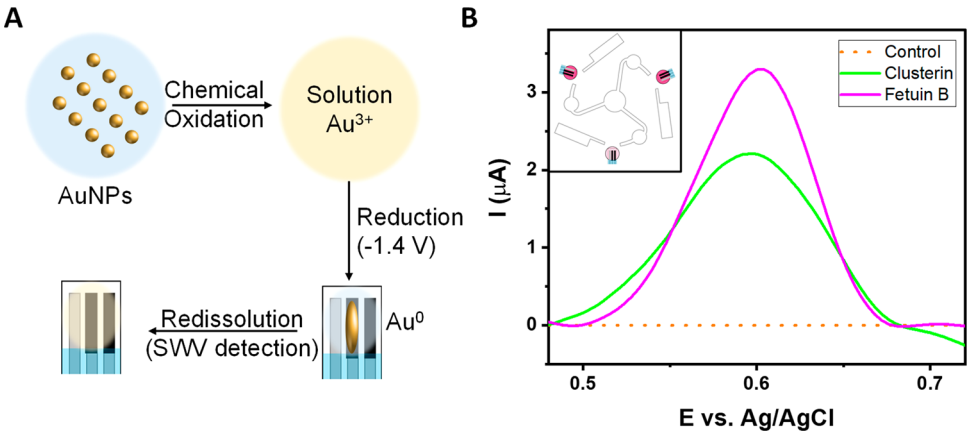

Figure 2. (A) Detection mechanism using HBr/Br_2 and redissolution voltammetry. (B) Screen-printed electrodes are positioned on top of the test zones (inset) and SWV measurements are performed for the biomarkers' quantification.

fetuin B and clusterin were detected in the presence of another proteic Alzheimer's biomarker related to alterations in the brain volume, pancreatic prohormone (PPY),[21,22] showing negligible interference of other present biomolecules. Due to the increased accessibility provided by the tests, these advancements hold considerable promise toward early-stage Alzheimer's disease diagnosis and understanding its developing mechanisms.

RESULTS AND DISCUSSION

A millimeter-size paper-based lateral flow immunoassay device has been developed (Figure 1A, i). The device consists of a central circle, corresponding to the sample zone (S) along with three independent arms. Each of them presents two more circles: one corresponding to the conjugate zone (C) and another to the test zone (T). The arm ends in a big rectangle, which acts as an absorbent zone (A) (Figure S1A). All the modified areas in the device are circular, assuring reproducible spreading of the solutions. Each path was modified with a specific AuNP-Ab conjugate, Ab(C) for clusterin and Ab(F) for fetuin B, for the quantification of the targeted biomarker (Figure 1A, ii). The third arm is unmodified and used as a control, remaining white after lateral flow of the sample. This device was designed with thin channels and soft curves, minimizing possible dead zones and allowing a continuous and homogeneous solution flow.

To obtain the best performance for the quantification of fetuin B and clusterin, two different strategies were applied. Fetuin B was detected using a sandwich approach (Figure 1A, iv). In this case, test zones were modified using anti-fetuin B antibodies Ab(F), and the pink color became more intense with increasing amounts of fetuin B on the sample. The use of this methodology was possible due to the multiple interaction sites for anti-fetuin B present on the protein. Clusterin, however, did not present simultaneous binding to two antibodies in the tested conditions. We hypothesize that the lack of multiple interaction sites between the protein and its specific antibody prevented a detectable signal. Therefore, a competitive assay was applied for clusterin (Figure 1A, iii). In this case, the analyte clusterin was immobilized on the test zones and competes with the clusterin contained in the sample for the interaction with antibody-labeled AuNPs. As a result, increasing concentrations of clusterin biomarker on the sample results in lighter pink tones (Figure 1B).

Fifteen minutes after sample addition, test zones were analyzed using both electrochemistry and colorimetric techniques. For colorimetric detection, test zone images were supplied to a customized software, which performed the automatic quantification of the biomarkers in CIE $L^*a^*b^*$ color space. The CIE $L^*a^*b^*$ was defined by the International Commission on Illumination (CIE) in 1976, and it expresses colors as three values: L^* indicates the lightness from black (0) to white (100), a^* from green (−) to red (+), and b^* from blue (−) to yellow (+).

Lateral flow devices were assembled and tested using anti-fetuin B antibodies in a sandwich immunoassay (Figure S2C). A solution containing 100 nmol/L of fetuin B and a blank sample (Tris-HCl buffer) were tested. In all cases, the sample homogeneously flowed through the three arms, with the test zone turning pink only in the presence of fetuin B (Figures 1C and S2C). Furthermore, AuNP-Ab conjugates were dragged with the solution flow, showing conjugate zones change color from pink to white color after sample application. No AuNP-Ab accumulation was visualized on the test zone after the application of blank samples. Good reproducibility among the arms was found for fetuin B (% RSD = 2.60, n = 3) when analyzing the colors using the parameter L^*.

Optimization of Lateral Flow Assay. Concentration, incubation times, and volume of solution were optimized for each of the lateral flow assay components. Respective data and figures are given in the Supporting Information (see Section S4), with the final protocol being described in the Methods section. The AuNP-Ab conjugation and protein immobilization onto the conjugate zone was also investigated (see Sections S2 and S3). Then, a calibration curve was constructed using fetuin B concentrations from 5 to 500 nmol/L, which includes its typical concentrations in human plasma (Table S2). The test zone displays more intense pink tones for higher protein concentrations, which are visible to the naked eye.

Choice of Detection Method. Biomarker quantification was performed *via* AuNP content on the testing pad. The AuNP quantification was performed by both electrochemistry and colorimetry methods. Electrochemical detection of biomarkers was performed by indirect determination of AuNP content. AuNP electrochemical quantification consisted in performing the oxidative dissolution of the NPs into metallic ions (Au^{3+}) for their further detection *via* square wave voltammetry (SWV) (Figure 2A). Figure 2B shows sample voltammograms for

DOI: 10.1021/acsnano.9b06571
ACS Nano XXXX, XXX, XXX−XXX

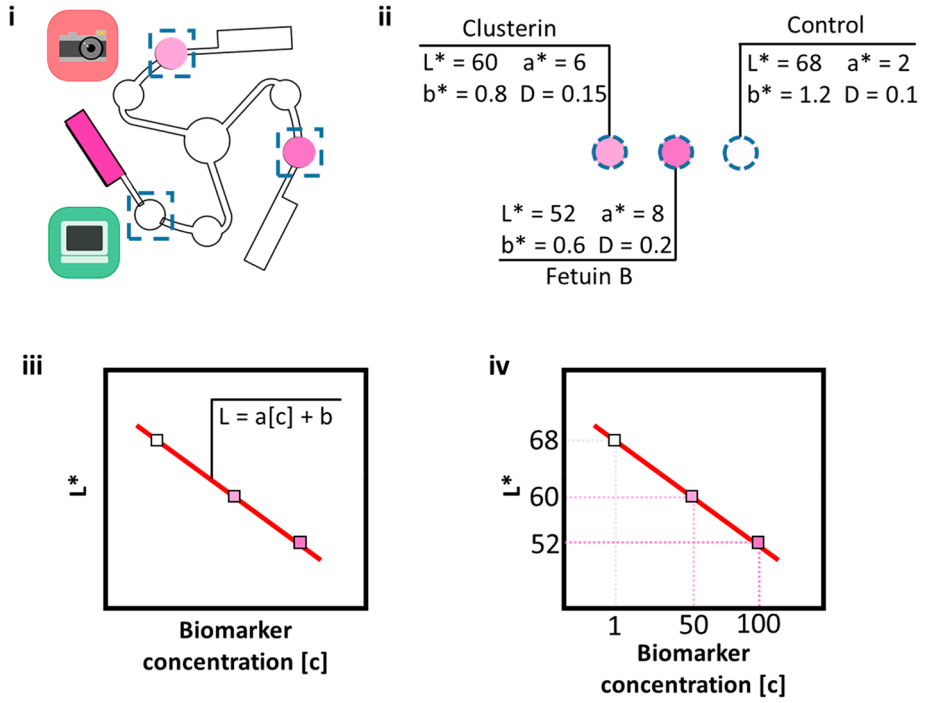

Figure 3. (i) Fifteen minutes after sample addition, first, pictures are taken, then, manually cropped on the dotted lines and provided to the developed software. (ii) Colorimetric software precisely segments the area to be analyzed and generates the color parameters *L**, *a**, *b**, and *D* for each test zone. Data for each biomarker are separated and, from there, the user can then follow two different paths. (iii) If the biomarkers' concentrations are known and provided to the software, a calibration curve is built. *L**, *a**, *b**, and *D* values for each of the analyzed points are provided to the users, as well as the linear regression equation. Or (iv) if the biomarkers' concentrations are unknown, a calibration curve can be loaded into the software. The program then returns the biomarkers' concentration based on the provided data, as well as a graph displaying the loaded calibration curve and the analyzed points. Colorimetric parameters *L**, *a**, *b**, and *D* for each test zone are also provided to the user.

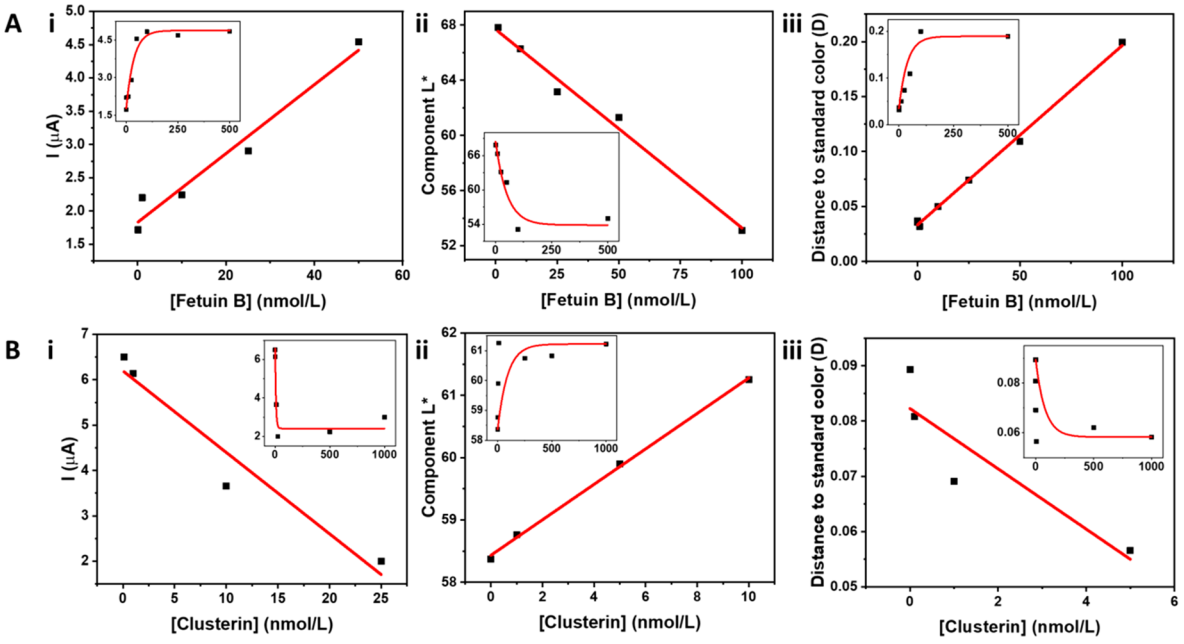

Figure 4. (A) Calibration curves for fetuin B using (i) electrochemical technique; (ii) colorimetric component "*L**", and (iii) colorimetric parameter "*D*". (B) Calibration curves for clusterin using (i) electrochemical technique; (b) colorimetric component "*L**", and (iii) colorimetric parameter "*D*".

clusterin and fetuin B using our customized screen printed electrodes (SPEs).

A good linearity was obtained (R^2 = 0.998) at concentrations from 10.48 to 104.77 μg/mL of AuNP-Ab (Figure S10A). Additionally, the sensor presented good sensitivity (0.143 μA mL/μg mm^2), and its LOD was calculated to be 0.32 ng/mL (Supporting Information S9). The fabricated SPEs displayed reproducibilities with a variation of RSD = 10.9% (n = 3), which were lower than commercial electrodes (RSD = 17.4%, n = 3).

DOI: 10.1021/acsnano.9b06571
ACS Nano XXXX, XXX, XXX−XXX

Colorimetric detection of biomarkers was performed by AuNP accumulation on the test zone, due to protein−antibody binding, changing the test zone color from white to pink. For the colorimetric analysis, a MATLAB-based software was developed. The program analyzes the intensity of pink tones present on the test zone and relates it to the AuNP-Ab concentration (Figure 3). The pictures are manually cropped and loaded into the developed software (i). Next, the algorithm performs a series of automated procedures and quantifies the AuNP-Ab. The colors of the image are treated to highlight the pink tones related to the label. Then, the software recognizes the areas to be analyzed and segments the image precisely (ii). The color tones are segmented into clusters according to their similarities. Accordingly, the value of each component on color space $L^*a^*b^*$ and the distance of the main cluster color to red are investigated (D). The user can then follow two different directions. If the sample concentrations are known and provided to the software, a calibration curve is generated (iii). If concentrations are unknown, a calibration curve can be provided to the program, and it determines the AuNP-Ab concentration (iv). The color analysis procedure was optimized to mitigate/reduce external noise in the colorimetric signal from background, shadows, or illumination without affecting the accuracy (see Section S8).

Biomarker Quantification Using the Lateral Flow Platform. The quantification of the studied biomarkers was performed using the lateral flow platforms and the AuNP-Ab optimized detection methods.

Calibration curves were constructed for each of the biomarkers individually. Fetuin B was explored from 0.1 to 500 nmol/L (Figure 4A and Figure S12A) using both colorimetric and electrochemical detection. Corresponding test zones and square wave voltammograms are displayed in Figure S11, respectively. Reproducibility and LOD of each parameter can be seen in Table 1, while R^2 and linear range can be seen in Table S8.

Table 1. RSD (%) and LOD for Each of the Biomarker Quantification Methods Tested (n = 3 Samples)

	fetuin B		clusterin	
method	RSD (%)	LOD (nmol/L)	RSD (%)	LOD (nmol/L)
colorimetry/L^*	2.79	0.24	1.82	0.12
colorimetry/a^*	20.26	0.09	21.07	0.03
colorimetry/b^*	17.83	1.77	25.43	0.70
colorimetry/D	21.67	0.09	20.39	0.03
SW voltammetry	17.27	0.003	25.76	0.0008

As expected from a sandwich assay, the higher the concentrations of fetuin B, the more intense the pink color obtained. Also, in all calibration curves, a linear tendency is followed by saturation. This probably occurs due to the limited number of interaction sites on the test zone, maintaining the obtained signal constant over determined protein concentration (100 nmol/L).

The linear range obtained using the different detection methods did not display significant variations between tested parameters, with typical concentrations being 0.1 to 100 nmol/L. However, additional analysis showed significant advantages and disadvantages of the compared methods. The colorimetric technique showed coefficients of linearity higher than those of the electrochemical technique (0.997 and 0.992 for D and a^* components, *versus* 0.960 for electrochemistry), while the electrochemical methods displayed a significantly lower LOD (0.003 nM for electrochemistry *vs* 0.09 nM for both colorimetric parameters "a^*" and D). Finally, the reproducibility of colorimetric parameter "L^*" stood out by being 10 times higher than the rest of the explored methodologies. Overall, the colorimetric parameter "L^*" was chosen to be the most useful parameter demonstrating good linear coefficients (0.988), good reproducibility (RSD = 2.79%, n = 3), and an adequate LOD of 0.24 nmol/L for detection of protein in human blood (typically found around 0.2 μmol/L[11,12]).

Similar studies were performed for clusterin for protein concentrations ranging from 0.1 to 1000 nmol/L (Figure 4B, Figure S12B) and analytical validation (Table 1 and Table S8). Square wave voltammograms and test zones can be found in Figure S11.

Clusterin calibration curves, similarly to fetuin B, displayed a linear tendency followed by saturation. In this case, the competitive format of analysis leads to a decrease in color intensity when increasing protein concentration. The saturation in this kind of system can be justified by the sample interaction with all available interaction sites on AuNP-Ab conjugates. When comparing electrochemical and colorimetric techniques, both present similar linearity values ranging from 0.1 to 25 nmol/L. Linear coefficients presented by colorimetric techniques (0.998 for "L^*" and 0.962 for "b^*") were higher than those of electrochemical techniques (0.945). Furthermore, LODs were significantly lower using electrochemistry (0.8 pmol/L) than using colorimetric techniques (0.12 and 0.7 nmol/L for "L^*" and "b^*", respectively). Again, a 10 times higher reproducibility for the "L^*" parameter when compared to other techniques was observed.

Therefore, the parameter "L^*" displayed the best overall performance for quantifying both biomarkers, showing high linearity coefficients and good reproducibility. This result is different than the one obtained on a standard calibration test performed during the absence of protein. In this case, "a^*" and "D" displayed the best results for AuNP-Ab quantification. This can be explained by the fact of AuNPs changing color by the presence of biomolecules, such as proteins, on the surface.[23] Furthermore, three different protein mixtures containing fetuin B, clusterin, and PPY were explored, indicating no significant cross-reactivity among the detection arms of the device (Table S9).

Therefore, the device is capable of simultaneously detecting AD biomarkers and displays a good potential for applications using complex samples such as plasma and/or other biological fluids.

CONCLUSIONS

We have described a lateral flow paper-based biosensor for the simultaneous quantification of two AD biomarkers (fetuin B and clusterin) using Ab-labeled AuNPs. The developed test design allows the usage of a 3-fold less volume of sample when compared to the conventional stick format and provides easy assembly and lowered production costs. The colorimetric methodology using parameter "L^*" displayed the best potential for biomarker quantification, showing good reproducibility and linearity. Furthermore, the biosensor displayed low rates of cross-reactivity in multianalyte samples. This device is also capable of quantifying AD biomarkers at normal blood levels. Thus, this platform holds great potential for assisting the Alzheimer's disease diagnosis and fast study of a larger amount

DOI: 10.1021/acsnano.9b06571
ACS Nano XXXX, XXX, XXX−XXX

of patients, making routine testing more accessible and therefore increasing use throughout the healthcare sector toward high probability of early detection.

With the goal of increasing the accessibility of the developed devices, future improvements may include substitution of professional cameras with personal mobile phones and relevant software/apps for automated analysis. Patterned colors can be added to the device, aiding the test zone analysis with different lightning and allowing users to perform the test in a wide range of scenarios. Further steps to assess real-world scenarios will be implemented by focusing on exploring biofluids from healthy and diagnosed patients. Furthermore, the developed device can be readily adapted for the multiple detection of innumerous other analytes and biomarkers, with added sensing branches if necessary for additional protein interferent analysis.

We foresee that our developed devices will have considerable potential for precise diagnosis of AD biomarkers in an accessible manner, which could eventually result in an enhanced life expectancy of AD patients and a better understanding of the disease mechanism, possibly toward improved therapies.

METHODS

Device Patterning. Microfluidic devices are composed by three individually cut parts (Figure S1A). (i) A 2 × 2 cm^2 wide release pad (Standard 14 Conjugate release pad, GE Healthcare, USA) that combines the sample (S) and conjugate (C) areas. This part was cut by a CO_2 laser cutter (40 W, Orion Motor Tech, at 1% of the maximum power). (ii) A 3 mm diameter test zone based on nitrocellulose (NC) (FF120HP PLUS, GE Healthcare, USA). Circular pads were cut with a manual pressure hole puncher (3EG, EDA, Brazil). Finally, (iii) an absorbent zone (A) composed by a thick cellulose membrane (CFSP173000, Merck Millipore, USA), which was cut with scissors.

Paper-Based Device Modification. Three different device areas are modified to ensure its proper functioning: (1) the test zone, which has specific bioreceptors being immobilized on its surface; (2) the conjugate zone, which has AuNP-Ab complexes that are able to move along with the sample flow; and (3) the sample zone, which is modified by Tween-20 to ensure uniform liquid flow.

The test area was modified by adding 1 μL of Ab (1 mg/mL, phosphate-buffered saline (PBS) 1×) for 15 min during constructing sandwich assays, as in the case of fetuin B, or by the modification by 3 μL of protein (0.25 mg/mL, PBS 1×) for 45 min, in the competitive assay, used for clusterin. Then, 10 μL of a BSA (bovine serum albumin) solution (1% w/v, PBS 1%, Sigma-Aldrich, USA) was incubated for 5 min to block any interaction sites available in the NC. Next, membranes were washed three times with PBS, dried with compressed air, and stored in a refrigerator until further use. Anti-fetuin B (11834-RP01) and anti-clusterin polyclonal antibodies (11297-RP01) were acquired from Sino Biological (China), as well as their antigens, fetuin B (11834-H08H) and clusterin (11297-H08H).

The conjugate zone was loaded with AuNP-Ab specific for each desired analyte. The conjugates were fabricated using an InnovaCoat Gold 20 nm kit, following precisely the manufacturer's instructions (Expedeon, England). For loading the conjugate zone, 2.5 μL of AuNP-Ab was added every 30 min up to 10 μL, at room temperature (24 °C). The device was completely dry and stored at 5 °C for further use.

Furthermore, the sample zone was modified with 10 μL of Tween-20 (0.1% v/v, Sigma-Aldrich, USA), to ensure uniform liquid flow through the device and left to dry at room temperature.

For the simultaneous biomarker quantification, one of the device's path was modified for fetuin B detection, the second for clusterin detection; the third path was used as a flux control, being coated only with BSA. The control path is expected not to present any color change after sample addition.

Assembly and Use of the Device. A polyethylene terephthalate (PET) substrate was used as a support for assembling the lateral flow device (Figure S1B). First, a 3.0 × 3.0 cm^2 PET was covered using double-sided tape. Then, three nonmodified NC membranes were attached using a mold. NC membranes were modified in the PET platform (i), and the main part (with conjugate zones already loaded with AuNP-Ab and sample zone modified by Tween-20) (ii) and absorbent zone (iii) were added to form the final device. The structures overlap by ∼0.5 mm, assuring uniform liquid flow between each piece. To perform the analysis, 50 μL of sample was added at the center of the device. Protein solutions were prepared in Tris-HCl (50 mM, pH 8.0, NaCl 150 mmol/L). Fifteen minutes after sample addition, quantification of biomarkers was performed using both electrochemical and colorimetric techniques.

Fabrication of Customized Screen-Printed Electrodes. Customized SPEs were fabricated using a semiautomatic printer, MMP-SPM (Speedline Technologies, USA), and tailored stencils. The stencils were designed using AutoCAD software (Autodesk, USA) and produced by Metal Etch Services (USA) using stainless steel sheets (30.5 × 30.5 cm^2). The electrodes were printed on PET in two different steps (Figure S1C). First, Ag/AgCl ink (E2414, Gwent Inc., UK) was used for printing the reference electrode, and three conductive trails were used for the electric connections. The printout was cured at 85 °C for 15 min. Then, carbon ink (C2070424P2, Gwent Inc., UK) was used to print the counter and working electrodes, and the layer was cured at 85 °C for 15 min. Next, a transparent insulating layer (Dupont 5036, USA) was used to define the electrode area of 3 mm^2 for the working electrode. Figure S1 Ci shows the final electrochemical design. Designs were optimized and tested according to their stability, reproducibility, and repeatability (Section S7), with the straight-electrode design showing the best performance.

Electrochemical Measurements. All electrochemical measurements were performed using customized SPEs in a μStat 200 potentiostat (Dropsens, Spain). To quantify the AuNPs after lateral flow tests, the metal was oxidized on the corresponding pad using an optimized acidic solution (see Section S5 for details). Fifteen minutes after sample addition, the paper-based channel adjacent to the test zone was disconnected to prevent any reaction products from diffusing throughout the paper device during electrochemical measurements. We then applied a 6 μL drop of a HBr/Br_2 mixture (1.0 M HBr, 0.1 mM Br_2, ultrapure water) (Sigma-Aldrich, Brazil) on the test zone for 15 min. Next, 0.5 μL of phenoxyacetic acid (1.0 mM, ultrapure water) (Sigma-Aldrich, Brazil) was added to the solution. Electrodes were put in contact with the soaked testing paper, and a SWV test was performed (Figure 2) using the following parameters: accumulation time:150 s, −1.4 V, equilibration time 15 s, potential window 0.0 to +0.75 V, step 4 mV, amplitude 25 mV, and frequency 15 Hz. (See Section S6 for more details.) The gold oxidation peak intensity (i_{ox}) was then used to quantify the metal. All electrochemical measurements were performed at room temperature. Under this optimized conditions, sensor performance was evaluated (Section S9). Total time for electrochemical analysis was 35 min.

Colorimetric Measurements. Colorimetric analysis was performed on pictures taken with a professional digital camera, Canon EOS 600D, 15 min after sample addition. This time was chosen to address the minimum time required for a complete flow of the sample through the test zone. Furthermore, allowing longer than 15 min resulted in uneven colors, hence hampering the analysis because of dryness of the sample pad. The camera was equipped with Canon EFS 18−55 mm lenses, and a flash ring was used to guarantee uniform and standardized illumination. The protocol applied for taking pictures is as follows: (a) the distance between focal plane and sample: 28 cm, (b) ISO 3200; (c) F-stop: f/5.6; (d) exposure time: 1/100 s. For image analysis, a customized code was developed using MATLAB (MathWorks) (Figure 3). The optimized parameters used for software image analysis included a cutoff radius of 0.3, which describes the test zone analysis area, and n = 3, which indicates the number of color clusters used on the test. Four different components were evaluated, L^* for the lightness from black to white, a^* from green to red, b^* from blue to yellow, and D for the distance of the main cluster color to red. The total time for colorimetric analysis was 20 min.

DOI: 10.1021/acsnano.9b06571
ACS Nano XXXX, XXX, XXX−XXX

ASSOCIATED CONTENT

Supporting Information

The Supporting Information is available free of charge on the ACS Publications website at DOI: 10.1021/acsnano.9b06571.

(S1) Fabrication of the lateral flow device; (S2) study of AuNP-Ab conjugation; (S3) immobilization of proteins on nitrocellulose; (S4) lateral flow assay optimization; (S5) approaches to measure electrochemically; (S6) optimization of AuNP quantification using HBr/Br_2; (S7) selection of customized SPE design; (S8) optimization of colorimetric technique; (S9) standard calibration using electrochemical and colorimetric technique; and (S10) biomarkers detection (PDF)

AUTHOR INFORMATION

Corresponding Authors

*E-mail: lais.brazaca@usp.br (L.C.B.).
*E-mail: zuco@ifsc.usp.br (V.Z.).

ORCID

Laís C. Brazaca: 0000-0002-0456-7552
Valtencir Zucolotto: 0000-0003-4307-3077

Notes

The authors declare no competing financial interest.

ACKNOWLEDGMENTS

The authors are grateful to São Paulo Research Foundation, FAPESP (grant nos. 2015/02623-0 2017/03779-0) and Conselho Nacional de Desenvolvimento Científico e Tecnológico, CNPq (grant no. 140625/2015-1) for financial support. We also would like to thank the researchers from Nanomedicine and Nanotoxicology Group and from Laboratory for Nanobioelectronics, especially J. R. Sempionatto and L. García-Carmona, for their continuous cooperation in our studies.

REFERENCES

(1) Alzheimer's society. What is Alzheimer's disease http://www.alzheimers.org.uk/site/scripts/documents_info.php?documentID=100 (accessed Jun 20, 2018).

(2) Mckhann, G. M.; Knopman, D. S.; Chertkow, H.; Hyman, B. T.; Jack, C. R.; Kawas, C. H.; Klunk, W. E.; Koroshetz, W. J.; Manly, J. J.; Mayeux, R.; Mohs, R. C.; Morris, J. C.; Rossor, M. N.; Scheltens, P.; Carrillo, M. C.; Thies, B.; Weintraub, S.; Phelps, C. H. The Diagnosis of Dementia Due to Alzheimer's Disease: Recommendations from the National Institute on Aging-Alzheimer's Association Workgroups on Diagnostic Guidelines for Alzheimer's Disease. *Alzheimer's Dementia* **2011**, *7*, 263−269.

(3) De Almeida, S. M.; Shumaker, S. D.; LeBlanc, S. K.; Delaney, P.; Marquie-Beck, J.; Ueland, S.; Alexander, T.; Ellis, R. J. Incidence of Post-Dural Puncture Headache in Research Volunteers. *Headache* **2011**, *51*, 1503−1510.

(4) Schneider, P.; Hampel, H.; Buerger, K. Biological Marker Candidates of Alzheimer's Disease in Blood, Plasma, and Serum. *CNS Neurosci. Ther.* **2009**, *15*, 358−374.

(5) Li, J.; Llano, D. a.; Ellis, T.; LeBlond, D.; Bhathena, A.; Jhee, S. S.; Ereshefsky, L.; Lenz, R.; Waring, J. F. Effect of Human Cerebrospinal Fluid Sampling Frequency on Amyloid-β Levels. *Alzheimer's Dementia* **2012**, *8*, 295−303.

(6) Sattlecker, M.; Kiddle, S. J.; Newhouse, S.; Proitsi, P.; Nelson, S.; Williams, S.; Johnston, C.; Killick, R.; Simmons, A.; Westman, E.; Hodges, A.; Soininen, H.; Kloszewska, I.; Mecocci, P.; Tsolaki, M.; Vellas, B.; Lovestone, S.; AddNeuroMed Consortium; Dobson, R. J. Alzheimer's Disease Biomarker Discovery Using SOMAscan Multiplexed Protein Technology. *Alzheimer's Dementia* **2014**, *10*, 724−734.

(7) Smith, E. R.; Nilforooshan, R.; Weaving, G.; Tabet, N. Plasma Fetuin-A Is Associated with the Severity of Cognitive Impairment in Mild-to-Moderate Alzheimer's Disease. *J. Alzheimer's Dis.* **2011**, *24*, 327−333.

(8) Thambisetty, M.; Simmons, A.; Velayudhan, L.; Hye, A.; Campbell, J.; Zhang, Y.; Wahlund, L. O.; Westman, E.; Kinsey, A.; Güntert, A.; Proitsi, P.; Powell, J.; Causevic, M.; Killick, R.; Lunnon, K.; Lynham, S.; Broadstock, M.; Choudhry, F.; Howlett, D. R.; Williams, R. J.; et al. Association of Plasma Clusterin Concentration with Severity, Pathology, and Progression in Alzheimer Disease. *Arch. Gen. Psychiatry* **2010**, *67*, 739−748.

(9) Schrijvers, E. M. C.; Koudstaal, P. J.; Hofman, A.; Breteler, M. M. B. Plasma Clusterin and the Risk of Alzheimer Disease. *JAMA, J. Am. Med. Assoc.* **2011**, *305*, 1322−1326.

(10) Harold, D.; Abraham, R.; Hollingworth, P.; Sims, R.; Gerrish, A.; Hamshere, M. L.; Pahwa, J. S.; Moskvina, V.; Dowzell, K.; Williams, A.; Jones, N.; Thomas, C.; Stretton, A.; Morgan, A. R.; Lovestone, S.; Powell, J.; Proitsi, P.; Lupton, M. K.; Brayne, C.; Rubinsztein, D. C.; et al. Genome-Wide Association Study Identifies Variants at CLU and PICALM Associated with Alzheimer's Disease. *Nat. Genet.* **2009**, *41*, 1088−1093.

(11) Diao, W. Q.; Shen, N.; Du, Y. P.; Liu, B. B.; Sun, X. Y.; Xu, M.; He, B. Fetuin-B (FETUB): A Plasma Biomarker Candidate Related to the Severity of Lung Function in COPD. *Sci. Rep.* **2016**, *6*, 30045.

(12) Dietzel, E.; Wessling, J.; Floehr, J.; Schafer, C.; Ensslen, S.; Denecke, B.; Rosing, B.; Neulen, J.; Veitinger, T.; Spehr, M.; Tropartz, T.; Tolba, R.; Renné, T.; Egert, A.; Schorle, H.; Gottenbusch, Y.; Hildebrand, A.; Yiallouros, I.; Stöcker, W.; Weiskirchen, R.; et al. Fetuin-B, a Liver-Derived Plasma Protein Is Essential for Fertilization. *Dev. Cell* **2013**, *25*, 106−112.

(13) Ou-Yang, M.-C. C.; Kuo, H.-C. C.; Lin, I.-C. C.; Sheen, J.-M. M.; Huang, F.-C. C.; Chen, C.-C. C.; Huang, Y.-H. H.; Lin, Y.-J. J.; Yu, H.-R. R. Plasma Clusterin Concentrations May Predict Resistance to Intravenous Immunoglobulin in Patients with Kawasaki Disease. *Sci. World J.* **2013**, *2013*, 5.

(14) Yamada, K.; Shibata, H.; Suzuki, K.; Citterio, D. Toward Practical Application of Paper-Based Microfluidics for Medical Diagnostics: State-of-the-Art and Challenges. *Lab Chip* **2017**, *17*, 1206−1249.

(15) Gong, M. M.; Sinton, D. Turning the Page: Advancing Paper-Based Microfluidics for Broad Diagnostic Application. *Chem. Rev.* **2017**, *117*, 8447−8480.

(16) Li, X.; Tian, J.; Shen, W. Quantitative Biomarker Assay with Microfluidic Paper-Based Analytical Devices. *Anal. Bioanal. Chem.* **2010**, *396*, 495−501.

(17) Martinez, A. W.; Phillips, S. T.; Whitesides, G. M.; Carrilho, E. Diagnostics for the Developing World: Microfluidic Paper-Based Analytical Devices. *Anal. Chem.* **2010**, *82*, 3−10.

(18) Mettakoonpitak, J.; Boehle, K.; Nantaphol, S.; Teengam, P.; Adkins, J. A.; Srisa-Art, M.; Henry, C. S. Electrochemistry on Paper-Based Analytical Devices: A Review. *Electroanalysis* **2016**, *28*, 1420−1436.

(19) Liang, L.; Su, M.; Li, L.; Lan, F.; Yang, G.; Ge, S.; Yu, J.; Song, X. Aptamer-Based Fluorescent and Visual Biosensor for Multiplexed Monitoring of Cancer Cells in Microfluidic Paper-Based Analytical Devices. *Sens. Actuators, B* **2016**, *229*, 347−354.

(20) Zhao, C.; Thuo, M. M.; Liu, X. A Microfluidic Paper-Based Electrochemical Biosensor Array for Multiplexed Detection of Metabolic Biomarkers. *Sci. Technol. Adv. Mater.* **2013**, *14*, 54402.

(21) Doecke, J. D.; Laws, S. M.; Faux, N. G.; Wilson, W.; Burnham, S. C.; Lam, C.-P. P.; Mondal, A.; Bedo, J.; Bush, A. I.; Brown, B.; De Ruyck, K.; Ellis, K. A.; Fowler, C.; Gupta, V. B.; Head, R.; Macaulay, S. L.; Pertile, K.; Rowe, C. C.; Rembach, A.; Rodrigues, M.; et al. Blood-Based Protein Biomarkers for Diagnosis of Alzheimer Disease. *Arch. Neurol.* **2012**, *69*, 1318−1325.

(22) Hu, W. T.; Holtzman, D. M.; Fagan, a. M.; Shaw, L. M.; Perrin, R.; Arnold, S. E.; Grossman, M.; Xiong, C.; Craig-Schapiro, R.; Clark, C. M.; Pickering, E.; Kuhn, M.; Chen, Y.; Van Deerlin, V. M.; McCluskey, L.; Elman, L.; Karlawish, J.; Chen-Plotkin, A.; Hurtig, H. I.;

DOI: 10.1021/acsnano.9b06571
ACS Nano XXXX, XXX, XXX−XXX

Siderowf, A.; et al. Plasma Multianalyte Profiling in Mild Cognitive Impairment and Alzheimer Disease. *Neurology* **2012**, *79*, 897−905.
(23) Jazayeri, M. H.; Aghaie, T.; Avan, A.; Vatankhah, A.; Ghaffari, M. R. S. Colorimetric Detection Based on Gold Nano Particles (GNPs): An Easy, Fast, Inexpensive, Low-Cost and Short Time Method in Detection of Analytes (Protein, DNA, and Ion). *Sens. Bio-Sens. Res.* **2018**, *20*, 1−8.

DOI: 10.1021/acsnano.9b06571
ACS Nano XXXX, XXX, XXX−XXX